Nonlin. Processes Geophys., 16, 373–380, 2009
www.nonlin-processes-geophys.net/16/373/2009/

Nonlinear Processes in Geophysics

Nonlinear electron acoustic structures generated on the high-potential side of a double layer

R. Pottelette and M. Berthomier

LPP-CNRS/INSU, 4 avenue de Neptune, 94107 Saint-Maur des Fossés, France

Received: 26 January 2009 – Revised: 8 April 2009 – Accepted: 14 April 2009 – Published: 30 April 2009

Abstract. High-time resolution measurements of the electron distribution function performed in the auroral upward current region reveals a large asymmetry between the low- and high-potential sides of a double-layer. The latter side is characterized by a large enhancement of a locally trapped electron population which corresponds to a significant part (∼up to 30%) of the total electron density. As compared to the background hot electron population, this trapped component has a very cold temperature in the direction parallel to the static magnetic field. Accordingly, the differential drift between the trapped and background hot electron populations generates high frequency electron acoustic waves in a direction quasi-parallel to the magnetic field. The density of the trapped electron population can be deduced from the frequency where the electron acoustic spectrum maximizes. In the auroral midcavity region, the electron acoustic waves may be modulated by an additional turbulence generated in the ion acoustic range thanks to the presence of a pre-accelerated ion beam located on the high-potential side of the double layer. Electron holes characterized by bipolar pulses in the electric field are sometimes detected in correlation with these electron acoustic wave packets.

1 Introduction

Electron acoustic waves (EAW) are known to contribute most to electrostatic high frequency noise excited in a two-component electron plasma when the density of the cold population is smaller than the density of the hot electrons. The real part of the dispersion relation of these waves is given by:

$$f_{ea}^2 = f_{pc}^2 \frac{1+3k_{ea}^2\lambda_{Dc}^2}{1+1/k_{ea}^2\lambda_{Dh}^2} \quad (1)$$

where λ_{Dc} and λ_{Dh} are the cold and hot electron Debye lengths, k_{ea} the wave number and f_{pc} the cold plasma frequency.

When the hot to cold temperature ratio becomes larger than 10, the electron acoustic mode becomes more excited than the Langmuir mode and can be considered as the principal high frequency mode of the plasma (Tokar and Gary, 1984; Singh and Lakhina, 2001). Under conditions of strong excitation and in the absence of simultaneously excited ion acoustic waves, the EAW readily evolve into electron acoustic solitons which propagate at a speed faster than the electron acoustic velocity v_{ea}.

Since the pioneer work by Dubouloz (1993), electron acoustic solitary structures have been extensively studied (Berthomier et al., 2000; Berthomier et al., 2003; Shukla et al., 2004; Singh and Lakhina, 2004; Kakad et al., 2007; Lakhina et al., 2008). Structures of this type leading to the formation of bipolar pulses in the electric field (generally identified as electron holes) have been detected in the Earth's magnetosphere. Evidence for them to exist has been accumulated in many regions preferentially where magnetic field-aligned currents are expected to flow: in the plasma sheet boundary layer (Matsumoto et al., 1994), in the auroral region (Ergun et al., 1998), at the magnetopause (Cattell et al., 2002), the bow shock ramp (Bale et al., 2002), and even in the magnetosheath (Pickett et al., 2003).

Usually, electron holes evolve in the interaction of hot and cold electron plasmas; they are known as nonlinear BGK modes (Omura et al., 1996; Muschietti et al., 1999, 2002). The property of two electron temperatures populations allows for electron acoustic turbulence which has similar properties as ion acoustic waves. In its nonlinear state, it therefore consists essentially of solitary waves leading to electron phase space holes generation with much lower threshold for excitation than ordinarily believed. EAW like Langmuir waves are high frequency density waves. They may become trapped and modulated by ion acoustic density perturbations leading to modulation and generation of electron acoustic envelope solitons. As we are going to demonstrate below this

Correspondence to: R. Pottelette
(raymond.pottelette@lpp.polytechnique.fr)

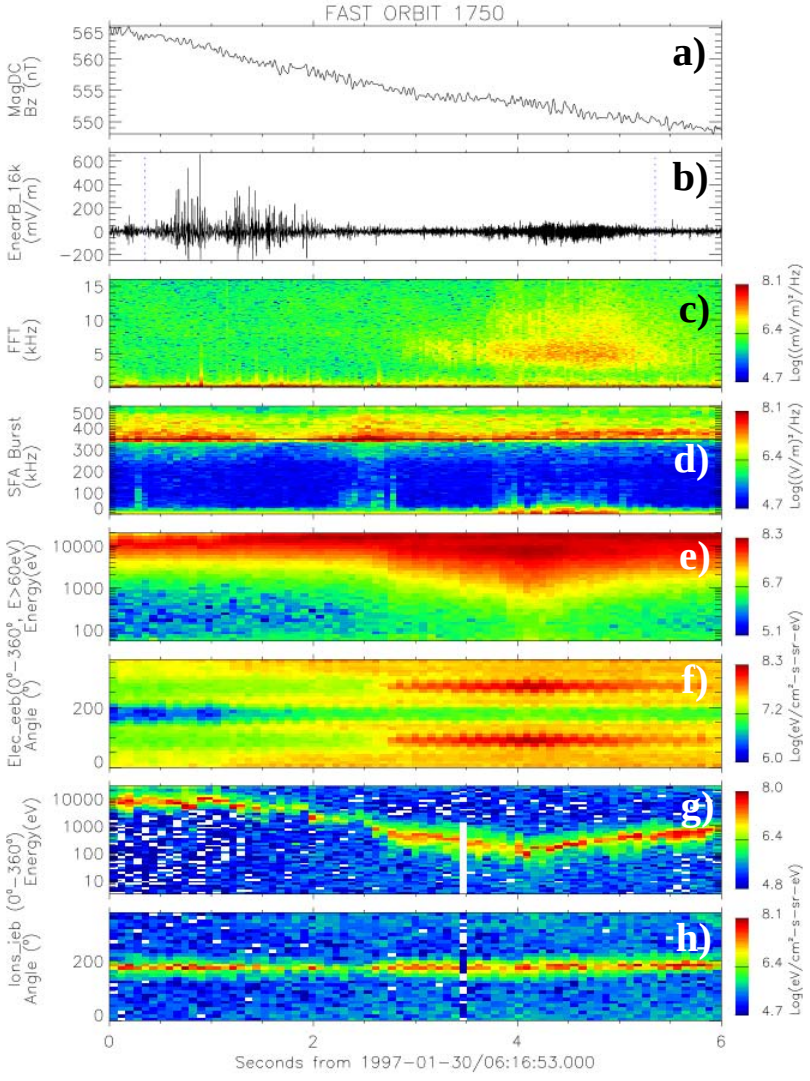

Fig. 1. The 6 s high resolution overview of the FAST auroral magnetosphere passage (orbit 1750) in the inverted-V anti-earthward current region described in the text: **(a)** magnetometer data. **(b)** 32 kHz waveform of the parallel electric field component. **(c)** Fourier transform of the parallel waveform. **(d)** Spectrum of the Auroral Kilometric Radiation generated near the electron gyrofrequency. **(e)** and **(f)** Electron energy flux and pitch angle distributions. **(g)** and **(h)** Ion energy flux and pitch angle distributions.

happens in the so-called auroral midcavity region (Ergun et al., 2004), when a pre-accelerated ion beam is located on the high-potential side of a double layer.

In the present paper, we use high-time resolution data from the FAST spacecraft in the auroral upward current region (Carlson et al., 1988). We show that – on the high-potential side of a double layer – the source of free energy for EAW lies in the difference in the parallel drift and temperature of the hot and trapped electron populations. The waves are mostly excited in a direction parallel to the magnetic field B where the temperature of the trapped population ($\sim$5 eV) is small as compared to that of the hot drifting electron population (several keV). As expected, the turbulent spectrum of the excited waves exhibits a maximum in the neighbourhood of the plasma frequency corresponding to the trapped electron population density.

2 Observations

Previous studies have indicated that the trapped electron population plays an important role by structuring the auroral parallel electric field (Ergun, 2004). In order to illustrate the systematic presence of such a population on the high-potential

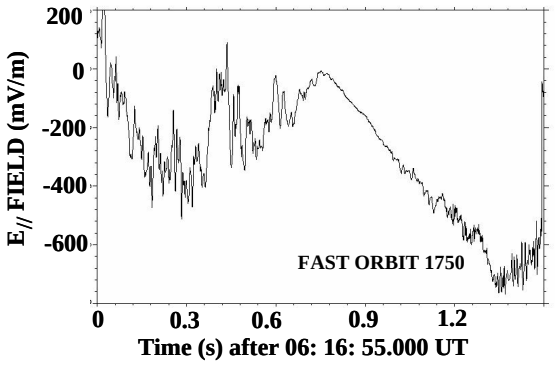

Fig. 2. DC electric field measurement during the time interval when particle acceleration processes take place. The parallel field exhibits a unipolar anti-earthward field typical for a potential ramp (double layer).

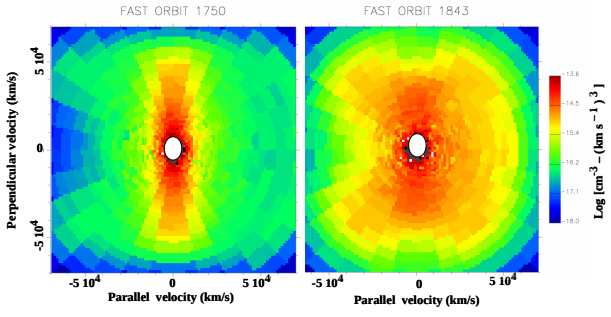

Fig. 3. Electron pitch angle distributions averaged over 300 ms at the times when a trapped electron population is measured in the high side of a double layer: Left: orbit 1750, Right: orbit ∼1843.

side of a double-layer, we have selected two FAST orbits, namely orbits 1750 and 1843. These orbits have been previously studied either in a somewhat different scientific context or we give in the present paper a new approach looking at the observations (Pottelette et al., 1999; Pottelette and Treumann, 2005).

2.1 Orbit 1750

The 6 s sequence of FAST particle and wave observations on 30 January 1997 at ∼22.30 MLT (orbit 1750) forming one basis of our discussion is shown in Fig. 1. FAST was on a poleward pass at invariant latitude ∼68° and altitude 4300 km. Panel a) shows it crossing the upward current region (negative magnetic field gradient). Electron energy flux and pitch angle distributions are given in panels e) and f), respectively. Before 06:16:55.000 UT the electrons form a downward beam, broadened toward larger pitch angles but with empty loss cone, typical for the presence of a parallel electric potential drop above the spacecraft. Starting from 06:16:55.000 UT, in about 1.5 s, the earthward parallel energy of the electron beam is accelerated from ∼10 to 20 keV. During this elapsed time, the entire ionospheric ion population (panel g) in the vicinity of the spacecraft is accelerated anti-earthward (180° in panel h) forming a cold ion beam with peak energy at about 10 keV. The ion pitch angle distribution does not show evidence for either down-going or a detectable low energy component. The entirety of these observations is consistent with the spacecraft crossing a localized region of ∼10 keV parallel potential drop.

From 06:16:55.000 UT, Fig. 2 shows the FAST spacecraft approaching and passing (during ∼1.5 s) a negative (upward directed) unipolar electric field ramp in a direction parallel to B. In this figure, the DC-coupled electric field fluctuations are sampled at ∼512 Hz; it can be seen that the parallel field reaches values ∼700 mV/m. As depicted in panel d) of Fig. 1, the presence of intense auroral kilometric radiation (AKR) generated near the electron gyro-frequency fce (black line at ∼340 kHz) indicates also that the spacecraft is in the auroral acceleration region.

We note that the spacecraft approaches the double layer from the low potential side. On the high potential side, starting from 06:16:56.000 UT, panel (f) indicates a large increase of electrons – at perpendicular pitch angles with well expressed peak fluxes at 90° and 270°. The left part of Fig. 3 displays the electron pitch angle distribution averaged over 300 ms during this time period. The trapped electrons are detected in the 1–10 keV energy range. Panels (b) and (c) of Fig. 1 show the 32 kHz waveform of the parallel electric component and its Fourier transform, respectively. A large increase in the wave activity is observed in correlation with the appearance of the trapped electron population. Broadband noise excitation in the kHz frequency range is clearly visible in panel (c) at the time when trapped energetic electrons are present. This broadband noise excitation is almost electrostatic as no measurable magnetic signal is detected.

The left part of Fig. 4 displays 20 ms of the waveform data covering this event, while in the right part we show the spectrum of these waves averaged over 300 ms. The electric field signal is dominated by a series of large amplitude (∼100 mV/m), strongly modulated coherent wave packets which are spatially periodic and have a recurrence period of ∼3 ms corresponding to waves of frequency ∼300 Hz, well in the hydrogen ion acoustic frequency range. Note the strong localization of the wave packets in time and space and their separation by gaps of nearly vanishing wave amplitude. Also note the strong monochromaticity of the high frequency waves trapped in the localized wave packets as indicated by the intense ∼6 kHz peak in the spectrum. During this event, the density of the energetic trapped electrons (in the 1–10 keV energy range) can be calculated from the electron spectrometer data. Selecting an opening angle of ±11° (experimental constraints) around the perpendicular to

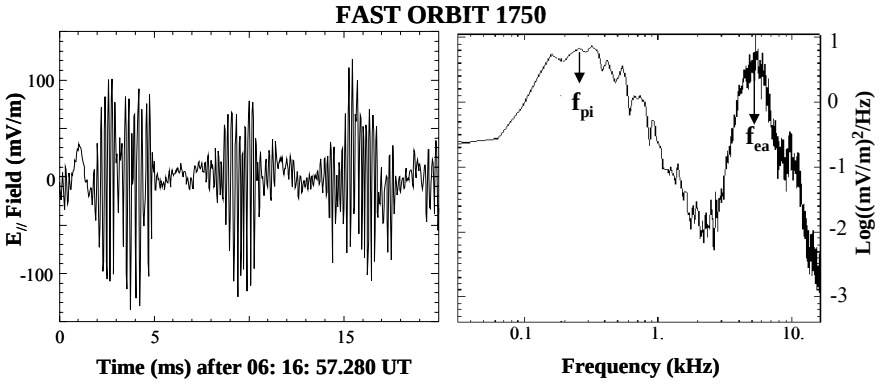

Fig. 4. Left: Waveform of broadband noise recorded during the time when a trapped electron population is present during orbit ∼1750. Right: Frequency spectrum showing the electron acoustic waves (at 6 kHz) and total plasma frequency (at ∼12 kHz) peaks. The broadband LF maximum near 300 Hz belongs to the ion acoustic wave spectrum.

B direction; this density amounts to 0.55 cm-^{3}. So, the 6 kHz emission line of the EAW spectrum can be safely interpreted as the plasma frequency f_p^t of the trapped electrons within a ∼10% accuracy. The total electron density peaks near $\sim 2\,\mathrm{cm}^{-3}$ corresponding to the weaker emission recorded at ∼12 kHz. It turns out that the density of the trapped electrons amounts to about 30% of the total electron density.

Four different particle populations can be identified on the high-potential side of the double layer. The first is the downward directed anisotropic energetic auroral electron beam (or electron conic) near 20 keV. This beam is fast, $v_b \sim 710^4\,\mathrm{km\,s}^{-1}$, and relatively dense $n_b \sim 0.0024\,\mathrm{cm}^{-3}$, which is about 0.1% of the total plasma density. Its distribution peaks parallel to the magnetic field and its parallel temperature is $T_{bll} \sim 1$ keV.

In addition to the electron beam, one has the hot auroral electron component with a parallel temperature $T_{hll} \sim 1$ keV comparable to the beam, and the trapped electron population with a weak parallel temperature $T_{tll} \sim 5$ eV. The hot electron component is moving downward at an average drift velocity $V_{Dh} \sim 1000\,\mathrm{kms}^{-1}$, this is substantially faster than the drift of the trapped component which is nearly standing. The ion beam, on the other hand, propagates upward at a speed of about $v_{bi} \sim 100\,\mathrm{kms}^{-1}$, while the temperature of the ions, taken from the spread of the distribution function is ∼200 eV. There are no cold background ions.

2.2 Orbit 1843

We show in this paragraph some data gathered by FAST during a rather similar event to the one previously studied. Fig. 5 collects a 6 s sequence of wave and particles data recorded throughout the upward current auroral region on 7 February 1997 at ∼2300 MLT. The spacecraft was at invariant latitude ∼66° and was travelling poleward at an altitude of 3950 km. The data exposed in panels (a) to (h) are of the same kind as those shown earlier in Fig. 1. Again, the presence of intense AKR emissions generated near the electron gyro-frequency (panel d) indicates that the spacecraft is in the auroral acceleration region, while the negative magnetic field gradient displayed in panel (a) characterizes the upward current region.

Starting from 20:50:12.000 UT, Fig. 6 shows FAST approaching and passing a negative unipolar parallel electric field ramp in the fluctuations sampled at ∼512 Hz of the DC-coupled electric field. The parallel field assumes values larger than $1\,\mathrm{V\,m}^{-1}$ in anti-earthward direction for roughly 0.5 s, being capable of accelerating electrons earthward and ions anti-earthward as observed. The simultaneously measured large perpendicular field corresponds to the crossing of a convergent electric field structure associated with an oblique double layer (Ergun et al., 2004). As seen in panels (e) and (g) of Fig. 5, in close connection with the detection of the double layer, the parallel energy of the ions drops from 4 keV to 200 eV, while the parallel energy of the electrons increases continuously from 4 keV to 8 keV. This fact provides strong support for the crossing of a localized parallel potential ramp of ∼4 keV amplitude.

On the high potential side of this double layer, starting from 20:50:12.700 UT, panel f) of Fig. 5 indicates a substantial increase of the electron density at perpendicular pitch angles in the 1–8 keV energy range. As compared to orbit 1750, the increase is however less pronounced and more distributed over pitch angles larger than 60° (see right part of Fig. 3). The density of the energetic trapped electrons (in the 1–8 keV energy range) calculated from the electron spectrometer data in an opening angle of ±11° around the perpendicular to B direction amounts to 0.25 cm-^{3}. This leads to $f_p^t \sim 4.5$ kHz for the characteristic plasma frequency of trapped electrons. On the other hand, the measured total electron density is $\sim 1.5\,\mathrm{cm}^{-3}$ corresponding to a plasma

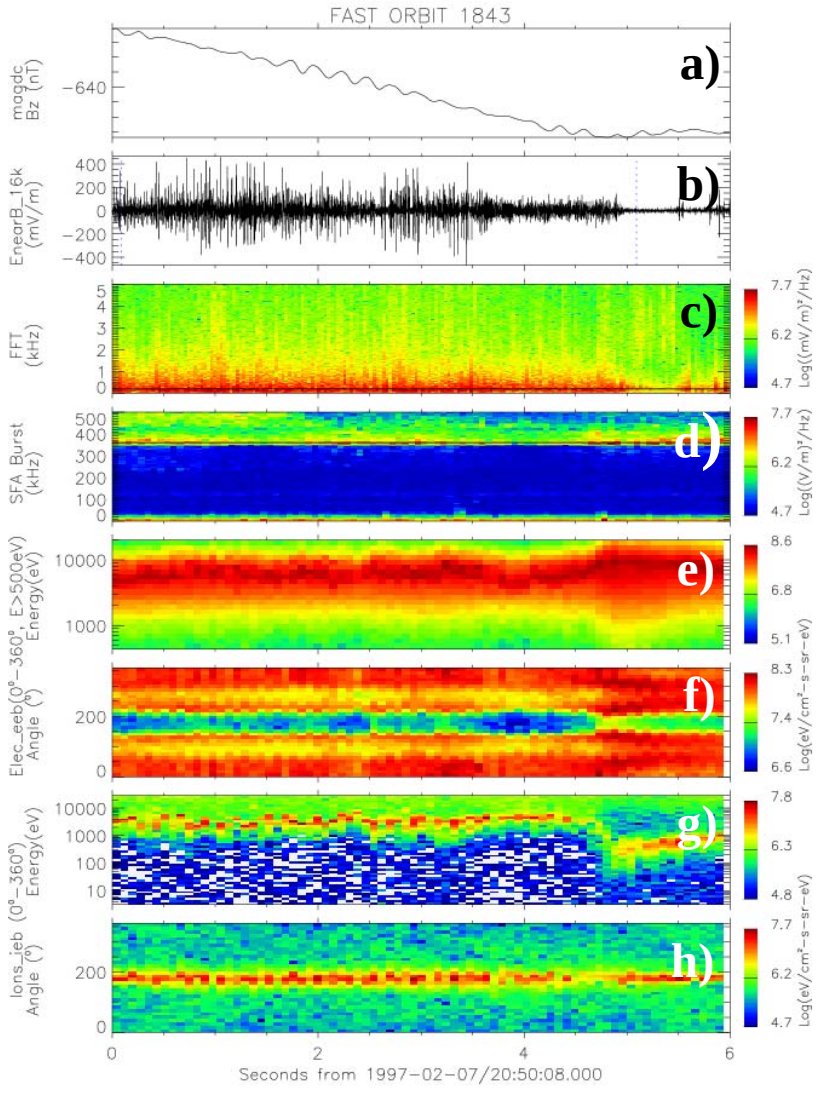

Fig. 5. Same data as in Fig. 1 but for orbit 1843: A 6 s high resolution overview in the inverted-V anti-earthward current region. The different panels are described in the text.

frequency of ∼11 kHz. In the present case, the density of the trapped population is about 20% of the total electron density.

Left part of Fig. 7 displays 20 ms of the waveform data covering this event, while the spectrum of the excited waves averaged over 300 ms is displayed in the right part. The waveform is dominated by a series of moderate amplitude (∼20 mV/m), strongly modulated coherent wave packets with a recurrence period of ∼4 ms. In the LF frequency range, the most excited frequency is located around 250 Hz corresponding to waves well in the hydrogen ion acoustic frequency range. A broadband secondary peak in the spectrum occurs in the 2–5 kHz frequency range. This latter corresponds to the plasma frequency range of trapped electrons and thus to the excitation of EAW. Note however that, as compared to orbit 1750, the excitation is weaker and occurs in a broader frequency range due to the fact that the electrons are more widely distributed around the perpendicular to **B** direction. The weaker emission recorded at ∼11 kHz matches with the total plasma frequency.

Again, as for orbit 1750, four different particle populations can be identified on the high-potential side of the double layer with different characteristics. The first is the downward directed anisotropic energetic auroral electron beam near 8 keV. This beam drifts with a parallel speed $v_b \sim 510^4$ km s^{-1}, its density is $n_b \sim 0.002$ cm $^{-3}$. Its distribution peaks parallel to the magnetic field and its parallel

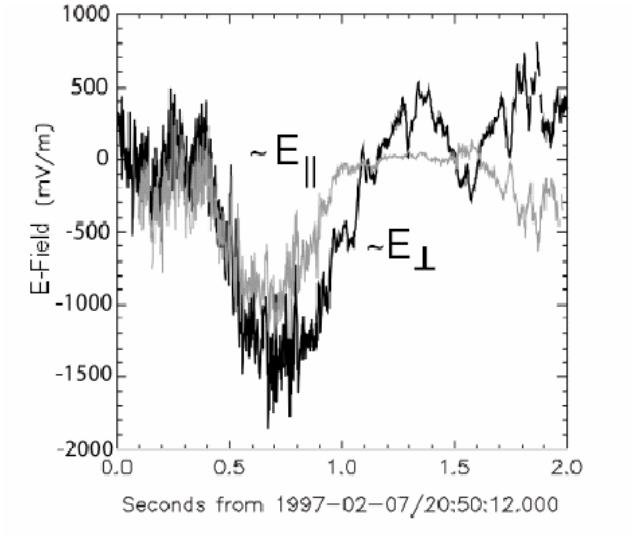

Fig. 6. DC electric field measurements for orbit 1843 during the same time interval in parallel (gray) and perpendicular (black) directions. The parallel field exhibits a unipolar anti-earthward field typical for a potential ramp (double layer).

temperature is T_{bll} ~1 keV.

The hot auroral electron component has a parallel temperatures T_{hll} ~1 keV comparable to the beam, while the parallel temperature of the trapped electron population is T_{tll} ~6 eV. The hot electron component is moving downward at an average drift velocity V_{Dh} ~1500 kms^{-1}, again substantially faster than the drift of the trapped component which is nearly standing. The ion beam, on the other hand, propagates upward at a speed of about v_{bi} ~100 kms^{-1}, while the temperature of the ions, taken from the spread of the distribution function is ~300 eV. In the present case, in addition to the ion beam, hot plasma sheet ions are present; their density is about 10% the ion beam density.

3 Discussion

Except for the auroral electron beam which excites the total plasma frequency, the three other particle components provide the free energy and the propagation conditions for ion and EAW. Figure 8 shows a sketch of their distribution functions. In the frame of the trapped electron distribution, the hot auroral electrons form a broad distribution centred at V_{Dh}. In order to determine the instability conditions for these waves, we take the following characteristic values for the main plasma parameters as derived from the measurements performed by the FAST spacecraft on the high-potential side of a double-layer: T_{hll} ~1 keV, T_{tll} ~5 eV, f_p^t ~6 kHz, f_{ph} ~10 kHz, f_{pi} ~300 Hz, V_{Dh} ~1000 kms^{-1}. This leads to λ_{Dt} ~20 m and to λ_{Dh} ~120 m for the values of the trapped and hot electron Debye lengths, respectively.

The excitation of the electron-acoustic waves is due to the drift of the hot electron component with respect to the background trapped electrons. The instability requires that $\boldsymbol{k}_{ea}.\ \boldsymbol{V}_{Dh} > 2\pi\ f_p^t$, where k_{ea} is the wave vector (Treumann and Baumjohann, 1996). In addition, the following inequality must be fulfilled $k_{ea}\lambda_{Dt} < 1$. Both inequalities lead to $3\,10^{-2} < k_{ea} < 5.10^{-2}$. Taking $k_{ea} \sim 4.\,10^{-2}$, one finds λ_{ea} ~150 m for the typical wavelength of EAW associated with a phase velocity $v_{ea} \approx$ 900 km/s. We have $k_{ea}\lambda_{Dh} > 1$, so the waves are generated in the short wavelengths limit where they become cold electron Langmuir waves as shown by Eq. (1). The trapped electron population, with its weak parallel electron temperature, plays indeed the role of the cold electron population with regard to waves excited parallel to B.

The excitation of ion acoustic waves can be understood when neglecting the cold trapped electrons. The condition for instability is that $V_{Dh} > c_{ia}$, where the ion acoustic velocity can be expressed in term of the electron to ion mass ratio and of the hot thermal velocity as $c_{ia} = V_h\ (m_e/m_i)^{1/2}$. With the typical plasma parameters defined above, we get c_{ia} ~300 km/s assuming that hydrogen is the main background ion species.

Since the ion beam is upward propagating in the opposite direction of the hot electrons the condition for instability is easily satisfied (see Fig. 8). The ion acoustic waves are excited in a broad range of phase velocities such that $c_{ia} < 2\pi f_{ia}/k_{ia} < V_{Dh}$. These waves can be excited up to the ion plasma frequency f_{pi}; their typical wavelength is of the order of a kilometre. In the fixed system of the Earth, the ion acoustic waves move downward together with the higher frequency EAW because their phase velocity is so close to V_{Dh}. We therefore end up with a situation where all the electrostatic waves are essentially moving down. In such a scenario the ion acoustic waves can both modulate and trap EAW to generate wave packets similar to the observed packets. Trapping is in principle possible up to any multiple half of the electron acoustic wavelength.

4 Conclusions

It has already been argued that double layers may be the dominant physical mechanism that supports the parallel field leading to auroral particles acceleration (Mozer and Hull, 2001). It should be emphasized that the characteristics of the turbulence generated on the low- and high- potential sides of a double layer appear very disparate (Pottelette and Treumann, 2005). From the FAST spacecraft observations we have inferred that:

1. EAW are generated on the high-potential side of a double layer, these observations enable to determine the density fraction of trapped electrons. In the absence of a retarding electric field these electrons would overwhelm

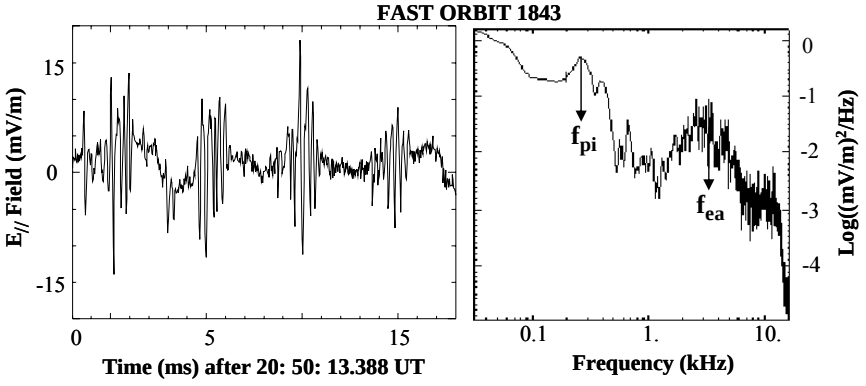

Fig. 7. Left: Waveform of broadband noise recorded during the time when a trapped electron population is present during orbit 1843. Right: Frequency spectrum showing the electron acoustic waves (at ∼4 kHz) and total plasma frequency (at ∼11 kHz) peaks. The broadband LF maximum near 250 Hz belongs to the ion acoustic wave spectrum.

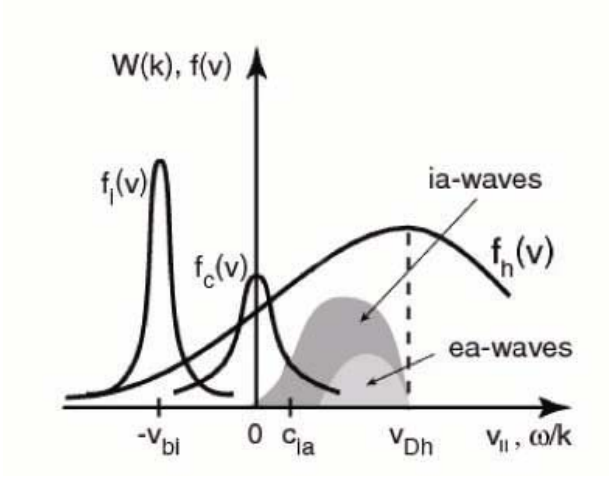

Fig. 8. Sketch of the particle distribution functions f(v) leaving out the auroral electron beam. Unstable spectra of electron and ion acoustic waves as function of ω/k are indicated by the shading. Both types of waves move downward in the cold (trapped) electron frame (After Pottelette et al., 1999, with permission by the American Geophysical Union).

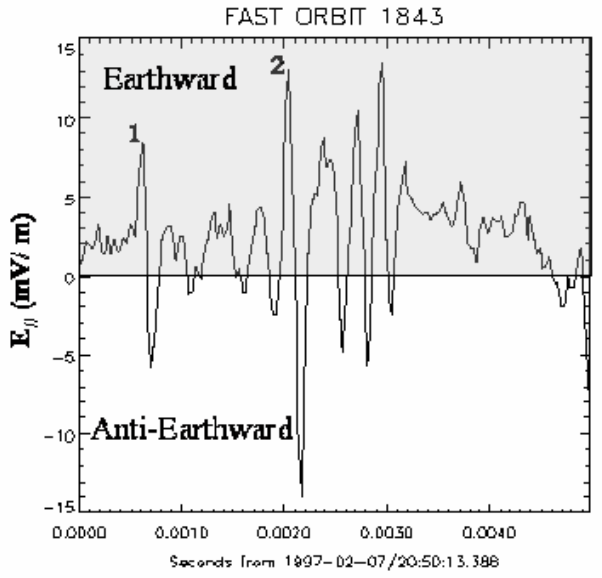

Fig. 9. Zoom of the left part of Fig. 7: High time resolution of the quasi-parallel electric field showing well defined bipolar electric field structures (labelled 1 and 2).

the auroral cavity. The trapped electrons resulting from velocity space diffusion account for a significant fraction of the local background electron density. As previously stated by Ergun et al. (2002), they appear to play an important role in determining the spatial distribution of auroral potential.

2. The EAW have typical parallel scales λ_{ea}∼150 m and are moving downward at a velocity of ∼1000 km/s. They are generated in the short wavelengths limit ($k_{ea}\lambda_{Dh}>1$) where they become cold electron Langmuir waves. The additional presence of ion acoustic turbulence excited by a weak energetic ion beam leads to the generation of modulated electron acoustic solitons.

3. The nonlinear excitation of the EAW may sometimes lead to the generation of electron holes. This is well illustrated by the 5 ms time sequence shown in Fig. 9 (which is an enlargement of the right part of Fig. 7) revealing the presence of well defined bipolar electric field structures (labelled 1 and 2) which reflect the presence of electron holes. This observation provides a convincing example regarding the possible non-

linear evolution of EAW into nonlinear structures similar to those described by BGK modes (Shukla et al., 2004).

4. The nonlinear EAW waves are the ultimate result of a parallel electric field in the upward auroral current region, they may, however, themselves self-consistently contribute to the generation of such large-scale parallel electric fields.

Acknowledgements. The FAST mission is a project of the Space Sciences Laboratory of the University of California at Berkeley run under the auspices of NASA. The authors are indebted to C. W. Carlson and R. E. Ergun for providing the particle and wave data as well as for some useful discussions. This research has been initiated within the France-Berkeley program.

Edited by: T. Passot
Reviewed by: G. S. Lakhina and another anonymous referee

The publication of this article is financed by CNRS-INSU.

References

Bale, S. D., Hull, A., Larson, D. E., Lin, R. P., Muschietti, L., Kellogg, P. J., Goetz, K., and Monson, S. J. : Electrostatic turbulence and Debye-scale structures associated with electron thermalization at collisionless shocks, Astrophys. J., 575, L25–L28, 2002.

Berthomier, M., Pottelette, R., Malingre, M., and Khotyaintsev, Y.: Electron-acoustic solitons in an electron-beam plasma system, Phys. Plasmas, 9, 2987–2994, 2000.

Berthomier, M., Pottelette, R., Muschietti, L., Roth, I., and Carlson, C.: Scaling of three dimensional electron phase space density holes observed by FAST in the auroral downward current region, Geophys. Res. Lett., 30(22), 2148–152, doi:10.1029/2003GL018491, 2003.

Carlson, C. W., Pfaff, R., and Watzin, J. G.: The Fast Auroral Snapshot (FAST) mission, Geophys. Res. Lett., 25, 2013–2016, 1998.

Cattell, C., Crumley, J., Dombeck, J., Wygan, J., and Mozer, F. S.: Polar observations of solitary waves at the Earth's magnetopause, Geophys. Res. Lett., 29(5), 1065, doi:10.1029/2001GL014046, 2002.

Dubouloz, N., Treumann, R. A., and Pottelette, R.: Turbulence generated by a gas of electron-acoustic solitons, J. Geophys. Res., 98, 17415–17422, 1993.

Ergun, R. E., Carlson, C. W., McFadden, J. P., et al.: FAST satellite observations of large amplitude solitary structures, Geophys. Res. Lett., 25, 2061–2064, 1998.

Ergun, R. E., Anderson, L., Main, L., Su, Y.-J., Newman, D. L., Goldman, M. V., Carlson, C. W., McFadden, J. P., and Mozer, F. S.: Parallel electric fields in the upward current region of the aurora: Numerical solutions, Phys. Plasmas, 9, 3695–3704, 2002.

Ergun, R. E., Anderson, L., Main, L., Su, Y.-J., Newman, D. L., Goldman, M. V. , Carlson, C. W., Hull, A. J., McFadden, J. P., and Mozer, F. S.: Auroral particle acceleration by strong double layers: The upward current region, J. Geophys. Res., 109, A12220, doi:10.1029/2004JA010545, 2004.

Kakad, A. P., Singh, S. V., Reddy, R. V., Lakhina, G. S., Tagare, S. G., and Verheest, F.: Generation mechanism for electron acoustic solitary waves, Phys. Plasmas, 14, 052305-9, doi:10.1063/1.2732176, 2007.

Lakhina, G. S., Kakad, A. P., Singh, S. V., and Verhest, F.: Ion- and electron-acoustic solitons in two temperature space plasmas, Phys. Plasmas, 15, 062903, doi:10.1063/1.2930469, 2008.

Matsumoto, H., Kojima, H., Miyatake, T., Omura, Y., Okada, M. et al.: Electrostatic solitary waves (ESW) in the magnetotail: BEN wave forms observed by GEOTAIL, Geophys. Res. Lett., 21, 2915–2918, 1994.

Mozer, F. S. and Hull, A.: Origin and geometry of upward parallel electric fields in the auroral acceleration region, J. Geophys. Res., 106, 5763–5775, 2001.

Muschietti, L., Ergun, R. E., Roth, I., Carlson, C. W.: Phase-space electron holes along magnetic field lines, Geophys. Res. Lett., 26(8), 1093–1096, 1999.

Muschietti, L., Roth, I., Carlson, C. W., and Berthomier, M.: Modeling stretched solitary waves along magnetic field lines, Nonlinear. Proc. Geoph., 9, 101–109, 2002.

Omura, Y., Matsumoto, H., Miyake, T., and Kojima, H.: Electron beam instabilities as generation mechanism of electrostatic solitary waves in the magnetotail, J. Geophys. Res., 101(A2), 2685–2697, 1996.

Pickett, J. S., Menietti, J. D., Gurnett, D. A., Tsurutani, B., Kintner, P. M., Klatt, E., and Balogh, A.: Solitary potential structures observed in the magnetosheath by the Cluster spacecraft, Nonlinear. Proc. Geoph., 10, 3–11, 2003.

Pottelette, R., Ergun, R. E., Treumann, R. A., Berthomier, M., Carlson, C., McFadden, J. P., and Roth, I.: Modulated electron acoustic waves in auroral density cavities: FAST Observations, Geophys. Res. Lett., 26, 2629–2632, 1999.

Pottelette, R. and Treumann, R.: Electron holes in the auroral upward current region, Geophys. Res. Lett., 32, L12104, doi:10.1029/2005GL022547, 2005.

Shukla, P. K., Mamun, A., and Eliasson, B.: 3-D electron acoustic solitary waves introduced by phase space electron vortices in magnetized space plasmas, Geophys. Res. Lett., 31, L07803, doi:10.1029/2004GL019533, 2004.

Singh, S. V. and Lakhina, G. S.: Generation of electron acoustic waves in the magnetosphere, Planet. Space Sci., 49, 107–114, 2001.

Singh, S. V. and Lakhina, G. S.: Electron acoustic solitary waves with non-thermal distribution of electrons, Nonlinear. Proc. Geoph., 11, 275–279, 2004.

Tokar, R. L. and Gary, S. P.: Electrostatic hiss and the beam driven electron acoustic instability in the dayside polar cusp, Geophys. Res. Lett., 11, 1180–1183, 1984.

Treumann, R. A. and Baumjohann, W.: Advanced Space Plasma Physics, Imperial College Press, London, UK, 82–84, 1997.